Astron. Astrophys. 316, 519–527 (1996)

ASTRONOMY
AND
ASTROPHYSICS

Ulysses COSPIN/LET: latitudinal gradients of anomalous cosmic ray O, N and Ne

K.J. Trattner[1]*, R.G. Marsden[1], V. Bothmer[1], T.R. Sanderson[1], K.-P. Wenzel[1], B. Klecker[2], and D. Hovestadt[2]

[1] Space Science Department of ESA, Postbus 299, 2200 AG Noordwijk, The Netherlands (trattner@estsck.estec.esa.nl)
[2] Max-Planck-Institut für extraterrestrische Physik, Postfach 1603, D-85740 Garching, Germany

Received 23 February 1996 / Accepted 20 May 1996

Abstract. A key goal of the Ulysses mission is the measurement of the latitudinal gradient of the Anomalous Cosmic Ray (ACR) component. Earlier studies using data from the COSPIN/LET experiment on board Ulysses together with in-ecliptic data from the HILT instrument on SAMPEX have shown a small (∼2% per degree) positive latitudinal gradient for anomalous oxygen in the energy range 8 to 16 MeV/n. This result is consistent with the effects of curvature and gradient drifts in the heliospheric magnetic field for the current polarity configuration: positively charged particles are expected to flow down to the heliographic equator from the polar regions.

In this paper we extend our previous work and include two additional ACR species, nitrogen (4 to 20 MeV/n) and neon (4 to 30 MeV/n). We also present our latest results on the ACR oxygen latitudinal gradient over an extended energy range (4 to 20 MeV/n). The period covered for all three species include the Ulysses south polar pass, the rapid transit from the south pole to the ecliptic and a significant portion of the climb to high northern latitudes. For all species and energy ranges the latitudinal gradients are between 1% and 2%, consistent with earlier studies, and show a slight tendency to larger gradients for higher magnetic rigidity.

Key words: interstellar medium: general – cosmic rays – interplanetary medium

1. Introduction

Ulysses has already successfully completed the first ever in-situ observations of the south and north polar regions of the sun (up to 80.2°). The main objective of the Ulysses mission (e.g., Page 1975, Marsden et al. 1986, Simpson 1989, Wenzel et al. 1989, Marsden et al. this issue) is to study the inner heliosphere in three dimensions. Before the Ulysses mission, in-situ observations of the heliosphere have been restricted to regions less than about 35° from the ecliptic plane. Among investigations of the latitudinal dependence of the magnetic field, solar wind, radio and plasma waves, solar X-ray emissions, interstellar neutral gas and dust (see Space Sci. Rev. 72, Nos. 1-2, 1995, Balogh 1995, Bothmer et al. 1995, Sanderson et al. 1995), the study of solar energetic particles and cosmic rays is one of the key subjects of the mission (e.g., Cummings et al. 1995a, Simpson et al. 1995a, Trattner et al. 1995a).

Previous observations of energetic particles in our solar system showed that these particles can be separated into three groups: Galactic Cosmic Rays (GCR), Solar Energetic Particles (SEP) and the Anomalous Component of Cosmic Rays (ACR). Compared with the other two components, the ACR shows an anomalous increase above the quiet time SEP and GCR particle spectra at energies below 50 MeV/n. Affected by this anomalous increase are species with high first ionization potential like He, N, O, Ne (e.g., Hovestadt et al. 1973, von Rosenvinge and McDonald 1975, Klecker 1977, Mewaldt et al. 1993, Hasebe et al. 1994) Ar and also small amounts of C (e.g., Cummings and Stone 1988). For example, while carbon and oxygen in SEP and GCR are almost equally abundant, oxygen exceeds carbon in abundance by about 30 to 1 in the 10 MeV/n ACR. In the energy range from 10 to 50 MeV/n there are also more alpha particles than protons in the ACR, while in GCR and SEP protons are typically $\geq$10 times more abundant than alpha particles. However, recent observations by Christian et al. (1995) and McDonald et al. (1995) have also firmly established the occurrence of ACR protons.

The apparent overabundance of elements with high first ionization potential led to the hypothesis that the source of the ACR is most probably the neutral interstellar gas (Fisk et al. 1974, Fisk 1986). These neutral particles are unaffected by the solar wind and due to their high first ionization potential penetrate into the inner heliosphere. On their way, a fraction becomes singly ionized by solar UV or by charge exchange with the solar wind. Such single ionized particles have been recently observed (e.g. Klecker et al. 1995). The ions are picked-up by the solar wind

Send offprint requests to: K.J. Trattner

* *Present address:* Mullard Space Science Laboratory, Holmbury St. Mary, Dorking, Surrey RH5 6NT, UK

(Möbius et al. 1985) and convected into the outer heliosphere where they may gain energy (10 to 100 MeV/n) due to shock acceleration at the solar wind termination shock (e.g., Pesses et al. 1981).

This model explains also the unusual composition of ACR. Atoms with higher ionization potentials like He, N, O and Ne are predominantly neutral in the interstellar medium and are able to reach the inner heliosphere more easily than atoms with lower ionization potentials. Once ionized, the trajectories of the singly-charged particles in the interplanetary medium depend in general on diffusion, convection with the solar wind, and drift processes (curvature and gradient drift) in the magnetic field. Depending on the magnetic topology, which also reverses in an 11-year cycle as the solar magnetic field reverses (e.g., Jokipii and Davila 1981), the ions drift either towards the pole or from the polar region. For the solar magnetic dipole polarity during the high latitude phase of Ulysses, modulation models that include gradient drifts predicted that positively charged cosmic ray particles would preferentially drift inwards and downwards from the heliospheric poles toward the equatorial zone (see, e.g., Jokipii 1977, Jokipii and Kota 1985, Potgieter 1985) which gives rise to radial and positive latitudinal intensity gradients. Negative charged particles, on the other hand, are predicted to drift inwards along the current sheet and drift polewards in latitude.

The intensities of both cosmic ray components, GCR and ACR, are strongly modulated by the solar activity. Forbush (1954) was the first who reported that variations of the cosmic ray intensity measured at the Earth are anti-correlated with the solar activity during the 11-year solar activity cycle. While the GCR intensity shows variations by about a factor of 10, the ACR intensity varies between solar maximum and minimum by at least a factor of 100. Due to these strong variations the ACR at 1 AU is only observable at solar minimum.

Previous studies of 10 and 14 MeV/n ACR oxygen at the current solar minimum (e.g., Cummings et al. 1995b, Trattner et al. 1995b) showed latitudinal gradients of $\sim$2%/degree. In this paper we extend our previous work on latitudinal gradients (Trattner et al. 1995a, Trattner et al. 1995b) to include in addition to oxygen two other species, ACR nitrogen (4 to 20 MeV/n) and neon (4 to 30 MeV/n). We also extend our previously used energy range for the ACR oxygen from 8 – 16 MeV/n to 4 – 20 MeV/n. The data set for all three species used in this study covers the Ulysses south polar pass, the rapid transit from the south pole to the ecliptic and a significant portion of the climb to high northern latitudes (up to about 75°N). The data obtained from Ulysses are compared with baseline observations from SAMPEX at 1 AU and with previous results.

2. Instrumentation and data selection

The analysis reported here is based on data from the Low Energy Telescope (LET), one of the five telescopes in the Cosmic Ray and Solar Particle Investigation (COSPIN) on board the Ulysses spacecraft (Simpson et al. 1992). The LET instrument measures the flux, energy spectra and elemental composition of solar energetic particles and low energy cosmic ray nuclei from hydrogen up to iron. The instrument covers an energy range from $\sim$1 to $\sim$75 MeV/n, using a double dE/dX vs. E solid-state detector telescope surrounded by a cylindrical plastic scintillator anticoincidence shield. The telescope geometrical factor, defined by two circular collimators, has a value of 0.58 cm^{2}sr for the coincidence channels. Low resolution single-detector measurements of protons and alpha particles are also made. In this case, the geometrical factor is $\sim$9.1 cm^{2}sr. The instrument produces two types of data: counting rate information for groups of particle species in several energy bands, and pulse height analysis (PHA) information permitting identification of the chemical species and energy of individual particles. All ACR analysis reported here is performed with PHA data.

Table 1. Ion species and Ulysses/LET energy ranges used in this study. Not all energy ranges have 1 AU baseline measurements from SAMPEX/HILT. These baselines are indicated by yes (Y) or no (N).

Ion	Energy range (MeV/n)	Baseline
Nitrogen	4 – 7	N
Nitrogen	8 – 20	Y
Oxygen	4 – 8	N
Oxygen	8 – 12	Y
Oxygen	12 – 16	Y
Oxygen	16 – 20	N
Neon	4 – 8	N
Neon	9 – 30	Y

The 1 AU baseline measurements used in this study have been provided by the Heavy Ion Large Telescope (HILT) on the SAMPEX spacecraft (Klecker et al. 1993). The HILT sensor has been designed to measure heavy ion elemental abundances, energy spectra, and direction of incidence in the mass range from helium to iron and in the energy range from 4 to 250 MeV/n. With its large geometrical factor of 60 cm^{2}sr the sensor is optimized to provide composition and spectral measurements for low intensity cosmic rays and for the anomalous component of cosmic rays. The instrument combines a drift chamber with a proportional counter system. The multi dE/dX vs. E technique provides a low background, mass and energy determination. The SAMPEX spacecraft was launched in July 1992 and operates in an 82° inclination, low Earth orbit (670 × 520 km).

The SAMPEX data at 1 AU are used as reference measurements to correct for the general increase of the ACR due to the decrease of solar activity. Since the position of Ulysses is changing, the effect of the radial gradient has to be taken into account in order to extract true latitudinal gradients. Previous observations (e.g., Webber et al. 1981) of ACR oxygen in the energy range of 9.5 to 23.5 MeV/n showed radial gradients of about 15%/AU from 1 to 15 AU. These authors used measurents at IMP 7 (I7), IMP 8 (I8) and Pioneer 10 (P10) for a data set in 1972 to 1980. Further observations of $\sim$7 to 25 MeV/n ACR oxygen by Cummings et al. (1990) for the time period 1987/1 - 183 showed different radial gradients in the inner and outer heliosphere. The average exponential gradients observed by I8, Voyager 1 (V1) and 2 (V2), Pioneer 10 (P10) and 11 (P11) were

about 14%/AU between 1 and 22 AU but only 3%/AU between 22 and 41 AU. Since an abrupt change of the radial gradient at a certain distance is rather unlikly, the authors used a power law fit to determine the radial dependence: $(1/j)(\partial j/\partial r) = 0.88r^{-0.96}$. Thus at 1 AU the differential gradient was 88%/AU. More recently, Cummings et al. (1995a) and Cummings et al. (1995b) showed for SAMPEX, V1, V2, P10 and Ulysses data the high variability of the ACR oxygen radial gradient at 10 MeV/n. By using a similar analysis as Cummings et al. (1990) they determined for the time period 1993/183-365 (radial range 1 to 58 AU) a radial dependence of $(1/j)(\partial j/\partial r) = 1.44r^{-1.7}$ while for the time period 1994/209-313 (radial range 1 to 61 AU) the radial dependence was $(1/j)(\partial j/\partial r) = 0.18r^{-0.7}$. This is equivalent to a radial gradient at 1 AU of 114%/AU and 18%/AU, respectively. Given the large variability in the measured radial gradient, we have adopted a value of 15%/AU to normalize the Ulysses data in the present study. We belive this choise is justified because, as discussed in Sect. 3, the latitudinal gradients we derived are rather insensitive to the value chosen.

Our data survey covers the period from August 1992 until July 1995. We use eight different energy ranges of nitrogen, oxygen and neon to calculate latitudinal gradients. A list of the energy ranges used in this study is shown in Table 1. For nitrogen and neon we use 20 day average intensities while for oxygen we use 10 day average values.

Not all energy ranges have corresponding baseline measurements from SAMPEX. To calculate latitudinal gradients also for those energy ranges we have extrapolated the available SAMPEX measurements in intensity, assuming a similar spectral form as measured at Ulysses (see detailed explanation in Sect. 3). To increase the statistics, especially for neon, we have not restricted our data set to solar quiet times in the case of Ulysses. Since we are in a solar minimum phase our energy channels, especially the higher ones, are not affected by solar energetic particles. Our analysis of plots of the full data set compared with solar quiet times plots showed almost no difference in intensity and are completely equivalent at higher latitudes when Ulysses was in the high speed solar wind. The only problematic periods are in 1992 and early 1993 when the sun's activity was still high. A detailed analysis of the individual spectra showed a contribution of solar energetic particles in the low energy channels used in this study. This effect has been considered for the determination of latitudinal gradients. Since SAMPEX is operating in a low earth orbit, only data accumulated over the poles (above 70°) have been used in this study. The SAMPEX data set was further restricted to solar quiet times to avoid contamination of the ACR measurements with energetic particles caused by, e.g. CIR's. These quiet times are carefully chosen by using only periods where the helium intensity in the energy range from 4 to 6 MeV/n are below 8×10^{-4} cts/cm^2 s sr MeV/n.

3. Results and discussion

We show in Fig. 1 oxygen, nitrogen and carbon spectra between 3 and 30 MeV/n for selected periods in 1991 (day 110 – 160) and in 1995 (day 170 – 320). The spectra for the solar active period in 1991 on the left side of Fig. 1 are power laws with the same spectral slope ($\gamma = -2.3$) for all three species. In contrast, the right side shows spectra for a quiet time period where Ulysses was at high northern latitudes. The intensities of the three species are significantly reduced due to the decreased solar activity. The spectral slope in the energy range of 4 to 10 MeV/n is about zero. The oxygen and nitrogen intensity are clearly enhanced compared to the carbon intensity, a characteristic signature of the anomalous component.

Fig. 2 shows 20–day average values of proton, oxygen and neon intensities over the complete Ulysses mission to day 274 of 1995 in the energy range from 4 to 8 MeV/n. Note that data acquired during the Jupiter flyby in February 1992 are not indicated in this plot. At launch in October 1990 and extending into 1991, solar activity was high. The particle intensity in this period, corresponding to solar maximum, shows spikes representing bursts of energetic particles accelerated by interplanetary travelling shocks and/or co-rotating interaction regions. The ACR is strongly modulated and completely masked by this solar activity. Starting in early 1992, these active periods become progressively weaker and less frequent. This decrease of solar activity is especially seen in the decrease of the proton intensity. However, even at high latitudes, energetic particle enhancements are observed. Only at the highest latitudes ($> 70°$) does the proton intensity drop to background values (see Sanderson et al. 1995). The intensity recovers during the ecliptic crossing and drops again at high northern latitudes. Oxygen and neon, on the other hand, show a different profile. During periods of high solar activity both components show similar increases to the protons, but as the solar activity decreases, the intensity in solar quiet periods starts to increase as a result of the ACR contribution. The important feature of the oxygen and neon intensity profiles is their continuous increase until the highest latitude is reached with a sharp drop in intensity during the passage of Ulysses through the ecliptic, followed by an increase in intensity on the way to high northern latitudes. This behaviour was reported in earlier studies (e.g., Trattner et al. 1995b) and was observed for all energy channels listed in Table 1. We expect such intensity variations in the case of a true ACR latitudinal gradient. Note that transient increases in the 4 to 8 MeV/n oxygen and neon fluxes can still be observed in 1993. This circumstance will be considered for the final calculation of ACR latitudinal gradients.

Fig. 3 shows a comparison of Ulysses and SAMPEX nitrogen data in the energy range from 8 to 20 MeV/n. The thin curve represents 20–day average values measured by the LET instrument onboard Ulysses while the bold curve shows data from the HILT instrument on SAMPEX. Also indicated (thin vertical lines) are the highest north and south latitudes reached by Ulysses and the ecliptic crossing. As in Fig. 2, the Ulysses data do not include the Jupiter flyby. The SAMPEX data have a data gap in early 1994 due to a shutdown of the HILT instrument. After the Jupiter flyby in February 1992, Ulysses started to climb to higher latitudes and moved closer to the sun. In late 1992, when Ulysses was at about 10°S, both instruments measured similar intensities. Both observed increases due to the decreasing solar modulation. However, comparison with the SAMPEX data

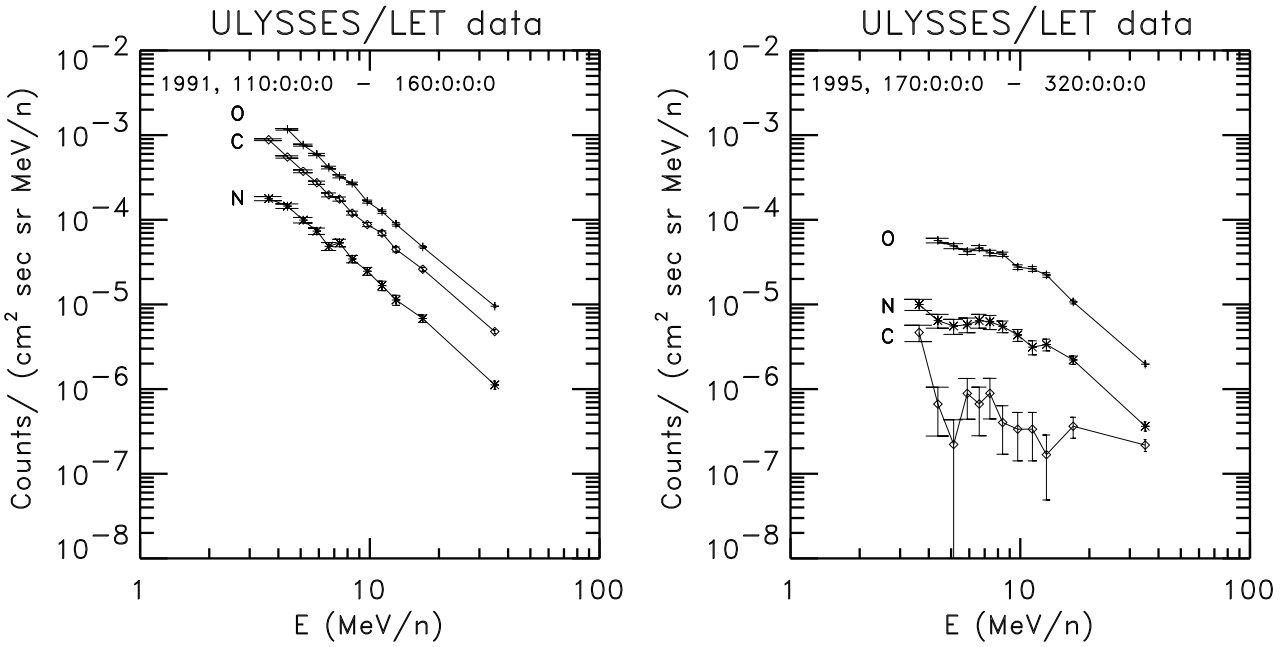

Fig. 1. Oxygen, nitrogen and carbon spectra for a solar active period in 1991 (left side) and the solar quiet north polar pass in 1995 (right side).

measured at 1 AU show that the two curves start to diverge after Ulysses moved beyond 30°S and only approach each other again after the maximum southern latitude was reached in September 1994. In March 1995, as Ulysses passed through the ecliptic plane, the HILT and LET instruments measured again similar intensities. The slightly higher intensity at the LET instrument is most probably a radial effect. During this time, Ulysses is still further out in the heliosphere than SAMPEX. After the ecliptic crossing, the intensity at Ulysses starts to rise again while the intensity at SAMPEX is more or less constant. The vertical line, which indicates the ecliptic crossing of Ulysses, shows that the minimum intensity was reached at about 18°S instead of in the ecliptic. This suggests that there is a significant asymmetry between the southern and the northern hemisphere. This observation was confirmed for all other energy ranges used in this study. However, the position of the flux minima vary with ion species. While the flux minima for neon are also at about 20°S, the oxygen flux minima are at about 10°S. This observation requires further studies.

As mentioned above, the SAMPEX data are used as reference measurements to correct for the overall increase of the ACR due to the decrease of solar activity. To determine the size of the latitudinal gradients we adopt the approach used in previous investigations (e.g., Bastian et al. 1979, McKibben et al. 1995, Trattner et al. 1995b) and perform least squares fits of the data to a function of the form

$$r_S = \frac{f_S}{f_U} = A \cdot \exp(G_r \cdot R + G_\Theta \cdot \Theta) \quad (1)$$

where r_S represents the SAMPEX/Ulysses flux ratio, R and Θ are heliocentric radius and heliocentric ecliptic latitude of Ulysses, G_r and G_Θ are the radial and latitudinal gradients and

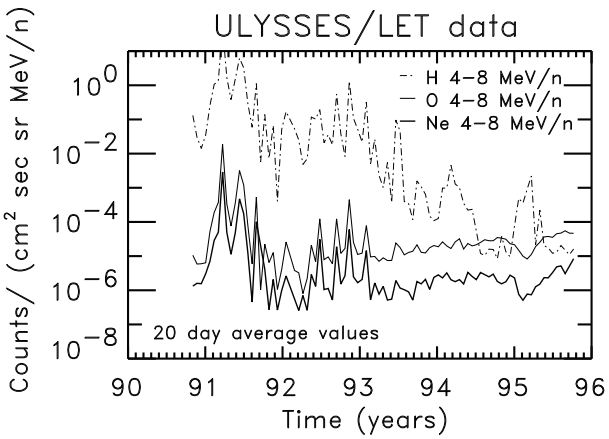

Fig. 2. 20-day average values of proton, oxygen and neon intensities (counts/cm^2 s sr MeV/n) in the energy range from 4 to 8 MeV/n, observed by Ulysses/LET.

A is a relative normalization determined by the fitting procedure. Least squares fits of the ratio r versus heliocentric ecliptic latitude will provide the latitudinal gradient G_Θ.

To compensate for radial gradients we used the results of previous studies with data acquired at the last solar minimum. As mentioned above, theories of particle acceleration which include curvature and gradient drifts in the large scale heliospheric magnetic field predict latitudinal and radial gradients of the cosmic rays. For a magnetic field directed inwards at the North pole (A<0), which was the case during the 1987 solar minimum, the particles gain access to the inner heliosphere along the neutral sheet. For a magnetic field directed inwards at the South pole (A>0) the particles flow down to the heliographic equator from

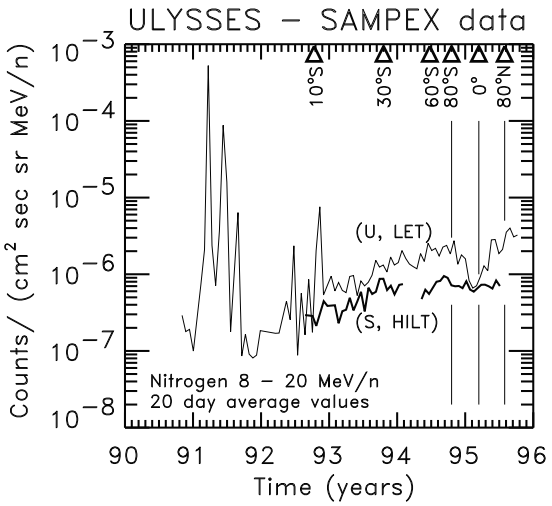

Fig. 3. 20–day average values of nitrogen intensities (counts/cm^2 s sr MeV/n) in the energy range from 8 to 20 MeV/n observed at Ulysses (U, LET) and SAMPEX (S, HILT).

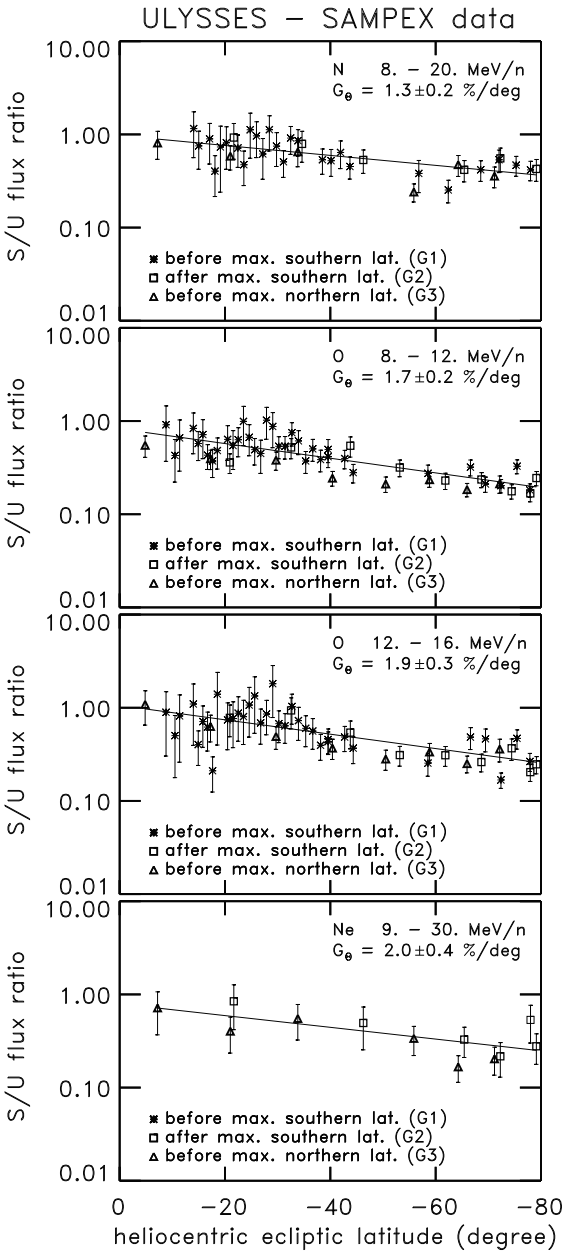

Fig. 4. SAMPEX to Ulysses flux ratio of nitrogen (8 to 20 MeV/n), oxygen (8 to 12 and 12 to 16 MeV/n) and neon (9 to 30 MeV/n) versus heliocentric ecliptic latitude. The straight lines indicating the trend are included to guide the eye.

the polar regions (Jokipii et al. 1977). This causes two observed effects: a latitudinal gradient which reverses sign between the two periods and a radial gradient which is smaller in the A>0 phase of the solar cycle. The average radial gradient (ACR oxygen at 10 MeV/n) between 1 and 61 AU during the current solar minimum is 2.6±0.6%/AU compared with 8.8±0.6% observed in 1987 between 1 and 41 AU (Cummings et al. 1995b). There are also reports of different radial gradients in the inner and outer heliosphere, e.g. during the last solar minimum in 1987 the average gradient was about 14%/AU between 1 and 22 AU but only 3%/AU between 22 and 40 AU (see Cummings et al. 1990). However, the actual radial gradient could be an even larger function of the radius in the inner heliosphere. Since no in-situ observations of radial gradients beween 1 and 5 AU for oxygen, nitrogen and neon are available we used a radial gradient of G_r = 15%/AU to normalize the Ulysses data to 1 AU. Note that the radial distance of Ulysses to the sun changed considerably before the south solar pass but was rather constant in the pole-to-pole segment of the trajectory. As our analysis shows that the radial correction of the Ulysses data does not significantly influence the value of the latitudinal gradients. Even for radial correction between 0%/AU – 30%/AU the latitudinal gradients remained within the error bars of our result reported below. In general, using a larger radial gradient would result in smaller latitudinal gradients.

Fig. 4 shows SAMPEX to Ulysses flux ratios for nitrogen (8 to 20 MeV/n), oxygen (8 to 12 and 12 to 16 MeV/n) and neon (9 to 30 MeV/n) versus heliocentric ecliptic latitude. Asterisks represent data before the maximum southern latitude while squares and triangles represent data after maximum southern latitude and before maximum northern latitude, respectively. The straight lines indicating the trend are included to guide the eye. For all data sets used in Fig. 4 a SAMPEX baseline in the same energy range was available. Our analysis showed that an unweighted fit through the complete data set is not an appropriate representation of the gradients. Fig. 3 above showed a significant asymmetry between the southern and northern hemisphere. The local flux minimum observed at Ulysses during its ecliptic pass occurred not at the ecliptic but at about 18°S. By plotting the data versus heliocentric ecliptic latitude, this asymmetry causes the SAMPEX to Ulysses flux ratios to be offset for the three data subsets corresponding to the south pole, the return to the ecliptic and to the north pole. Examples of this behaviour are seen in the bottom panel of Fig. 4 (Neon 9 to 30 MeV/n) and the top two panels in Fig. 5. While triangles in Figs. 4 and

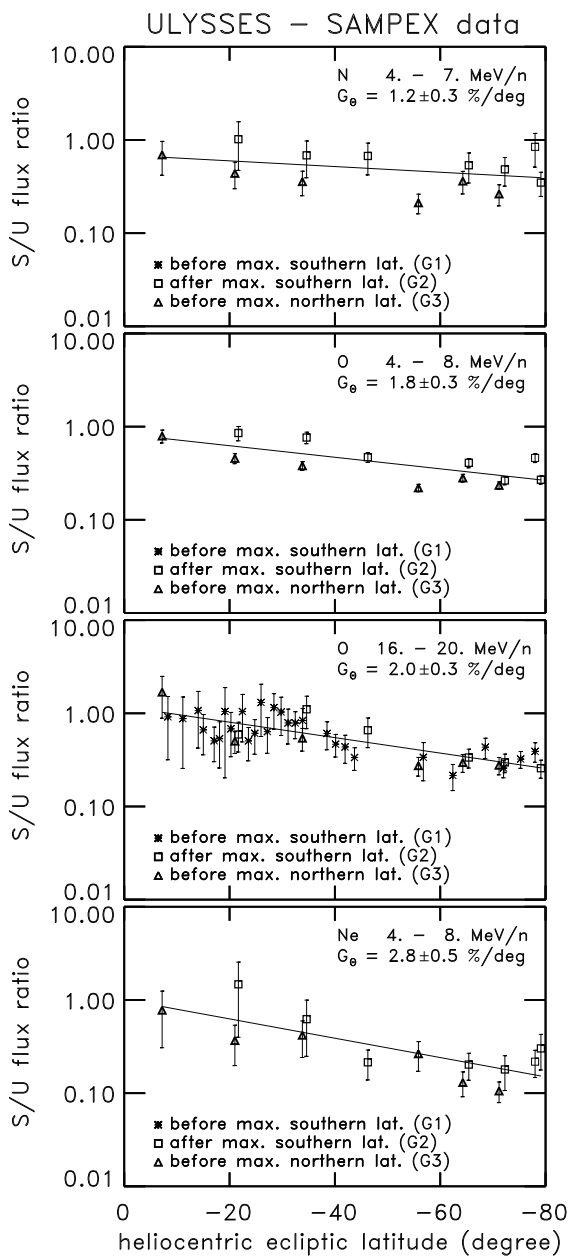

Fig. 5. SAMPEX to Ulysses flux ratio of nitrogen (4 to 7 MeV/n), oxygen (4 to 8 and 16 to 20 MeV/n) and neon (4 to 8 MeV/n) versus heliocentric ecliptic latitude. The straight lines indicating the trend are included to guide the eye.

5 are predominantly below the solid line, the squares are above it. Therefore the gradient calculation is strongly affected by the asymmetry. To avoid such an influence and to determine accurate results on the true latitudinal gradients we have separated the data set into three subsets.

- G1: ∼10°S – 80°S
- G2: 80°S – 0°
- G3: 0° – ∼75°N

This separation is consistent with the symbols used in Figs. 4 and 5. Latitudinal gradients have been calculated for each set. The final gradient for the different ion species and energy ranges, which is indicated in the panels in Figs. 4 and 5, is an average of the three individual gradients.

In addition, we have suppressed the G1 subset for the neon 9 to 30 MeV/n energy range. Since this was the time when the sun's activity began to decline and the ACR recovered, the count rate for neon was still so low that no significant fit could be established.

The average latitudinal gradients for the species and energy ranges in Fig. 4 are listed in Table 2. The gradients are between 1% and 2% per degree with a tendency for larger gradients for higher rigidities.

Fig. 5 shows SAMPEX to Ulysses flux ratios versus heliocentric ecliptic latitude for the other four channels in our study, nitrogen (4 to 7 MeV/n), oxygen (4 to 8 and 16 to 20 MeV/n) and neon (4 to 8 MeV/n). As in Fig. 4, the straight lines are to guide the eye. Asterisks again represent data before the maximum southern latitude while squares and triangles represent data after maximum southern latitude and before maximum northern latitude, respectively. As mentioned above, the sun still shows active periods up to the start of 1993. For the low energy channels in our survey (4 to 8 MeV/n and 4 to 7 MeV/n), this causes a significant contribution of solar energetic particles in addition to the ACR. We therefore also suppressed the G1 subset for the low energy channels in our survey. For the four data sets in Fig. 5 no SAMPEX baseline in the same energy range was available. To calculate these SAMPEX to Ulysses flux ratios we have extrapolated the known SAMPEX measurements. By plotting Ulysses data sets for the individual species N, O and Ne on top of each other we found that in general variations of the intensity curves are very similar. To avoid latitudinal effects on the extrapolation, we used data from the ecliptic crossing in March 1995 to calculate ratios of the known Ulysses intensities, i.e., oxygen (4 to 8 MeV/n) to oxygen (8 to 12 MeV/n). This ratio was used to extrapolate the SAMPEX oxygen curve (8 to 12 MeV/n) to 4 to 8 MeV/n. This method was also used to determine baselines for the other three channels. This method assumes that the spectral evolution of N, O and Ne at Ulysses and SAMPEX is the same, which should hold for times during solar minimum conditions. The only problematic times are in 1992 and 1993 when the solar activity was decreasing but still high. For these times the low energy channels in our survey see in addition to the rise of the ACR intensity also the presence of solar energetic particles (see the intensity peaks in Fig. 2). However, these G1 periods have been already excluded from our low energy channel surveys.

The average latitudinal gradients for the species and energy ranges in Fig. 5 are also summarized in Table 2. As in the case of the data in Fig. 4, these energy channels show latitudinal gradients of about 2% per degree with the tendency to larger gradients for higher rigidities. Also listed are the individual gradients for the subperiods G1, G2 and G3 and the corresponding magnetic rigidities (MV) for the energy channels used in this study. In agreement with predictions for the current polarity of the heliospheric magnetic field (positive northern fields), the intensities measured by Ulysses show positive latitudinal gradients. This

Table 2. Summary of latitudinal gradients for nitrogen, oxygen and neon. The gradients have been calculated separately for intensities observed by Ulysses/LET during the way to the south pole of the sun (G1), back to the ecliptic (G2) and up to the north pole (G3). GS represents gradients calculated by using an average value of the individual gradients.

Ion	Nitrogen		Oxygen				Neon	
(MeV/n)	4 – 7	8 –20	4 – 8	8 – 12	12 – 16	16 – 20	4 – 8	9 – 30
R (MV)	1432	2285	1710	2207	2611	2961	2137	3852
G1	-	1.4±0.3	-	1.9±0.3	1.5±0.5	1.9±0.3	-	-
G2	1.0±0.5	1.2±0.3	1.8±0.4	1.8±0.4	2.2±0.4	1.9±0.6	2.8±0.9	1.9±0.7
G3	1.3±0.4	1.3±0.5	1.8±0.3	1.5±0.2	1.8±0.4	2.4±0.6	2.8±0.5	2.0±0.5
GS	1.2±0.3	1.3±0.2	1.8±0.3	1.7±0.2	1.9±0.3	2.0±0.3	2.8±0.5	2.0±0.4

result suggests that the ACR enter the heliosphere at the current solar minimum via the solar poles and drift down to the ecliptic. Our results suggest that the individual species used in this study seem to have characteristic latitudinal gradients. While nitrogen has G_Θ =1.2%/degree, oxygen shows an average latitudinal gradient of about G_Θ = 1.8%/degree and neon of about G_Θ = 2.0%/degree. Note however, that the neon result has quite large error bars due to the low count rate.

Recent studies of latitudinal gradients for ACR helium and oxygen by Stone et al. (1987), Cummings and Stone (1988) and Cummings et al. (1990) with data of five spacecraft (IMP 8, V1, V2, P11 and P10) found a negative latitudinal gradient for the reverse solar magnetic polarity during the last solar minimum. In addition, Cummings et al. (1990) found that the latitudinal gradient of the ACR oxygen (7 to 25 MeV/n) in the outer heliosphere (data normalized to 30AU) is a function of the tilt angle of the neutral sheet. The maximum gradient of –5.5%/degree was reached during the last solar minimum period in mid–1987 when the tilt reached its minimum value of 9°. The absolute value of this latitudinal gradient is larger than the about 2% obtained in our investigation. However, these measurements were limited to 30° heliographic equatorial latitude and took place much further out in the heliosphere than the Ulysses measurements. The reverse magnetic polarity during that time caused an inward drift of the ACR in the neutral sheet of the heliosphere and from there a drift to higher latitudes. Both results are therefore consistent with theory and our results.

Our result is also in agreement with an observation from the current solar minimum by Cummings et al. (1995b) who found for ACR oxygen at 10 MeV/n a positive latitudinal gradient of 2.1±0.6%/degree. Their multispacecraft observations used data from Ulysses, SAMPEX, Pioneer 10, Voyagers 1 and 2, normalized to 30 AU. A similar result was determined by Trattner et al. (1995b) for oxygen 8 to 12 MeV/n and 12 to 16 MeV/n. These authors used a Ulysses data set which included the south solar pass down to a latitude of about 38°S. This restricted data set, normalized to 1 AU with G_r =15%, showed within their error bars almost the same positive latitudinal gradients of 2.1±0.3%/degree (8 to 12 MeV/n) and 1.6±0.9%/degree (12 to 16 MeV/n) as the present study.

Another feature which should be emphasized is that the data subset G1, corresponding to the period before the maximum southern latitude, actually showed no latitudinal gradient until Ulysses reached about 30°S (see Figs. 4 and 5). This feature was also mentioned by earlier studies (e.g., Trattner et al. 1995b) and is probably related to the configuration of the heliosphere at that time. Bame et al. (1993) showed that until Ulysses reached about 30°S latitude, the spacecraft was alternately exposed to the solar wind from the streamer belt and the polar coronal hole once per solar rotation. This was caused by the combined effect of the rotation of the tilted heliospheric current sheet and the equatorward extension of the coronal hole. However, the flux ratios for the subsets G2 and G3 (squares and triangles in Figs. 4 and 5) do not show such a behavior at low latitudes. These subsets show constant latitudinal gradients over the whole latitudinal range. In 1992 and 1993, before the maximum southern latitude was reached, the sun's activity started to decline and the ACR recovered. During that time the count rates were still low. As seen in Fig. 4 and 5, the Asterisks below 30°S show much larger error bars compared to the measurements at higher latitudes, or the squares and triangles. By the time of the fast latitude scan, Ulysses was already experiencing solar minimum conditions. In addition, it moved into the streamer belt at lower latitude compared with the crossing en route to high southern latitudes: about 22°S (Phillips et al. 1995), while the tilt angle of the current sheet was reported to be about ±10°–15° (Smith et al. 1995). As mentioned above, an influence of the tilt angle of the current sheet to radial and latitudinal gradients in the outer heliosphere (>30 AU) was reported by Cummings et al. (1990). The gradients appear to be correlated with the tilt angle of the current sheet. Furthermore, the heliosphere was in a more quiet and stable condition for the G2 and G3 periods than during G1. In summary, the later epoch is characterised by latitudinal gradients that have fully developed and a smaller tilt of the current sheet, enabling stable latitudinal gradients to be found for the complete latitudinal range.

4. Summary and conclusions

The Ulysses mission provides a unique opportunity to investigate the heliosphere in three dimensions. In this paper we have expanded our previous work (Trattner et al. 1995b) on latitudinal gradients of anomalous cosmic ray oxygen to include the additional ACR species nitrogen (4 to 20 MeV/n) and neon (4

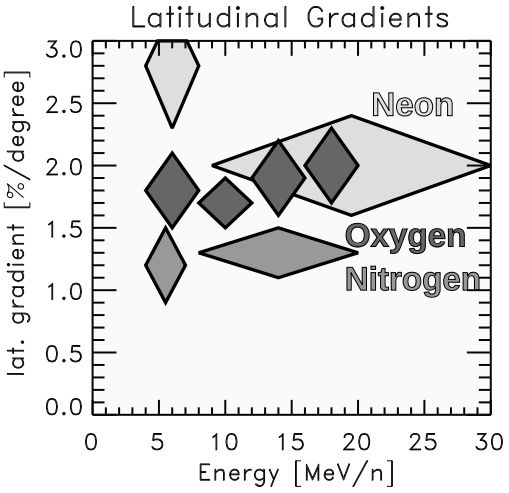

Fig. 6. Summary of latitudinal gradients of nitrogen, oxygen and neon. The listed gradients have been calculated by averaging individual latitudinal gradients for three data subsets to the maximum southern latitude (G1), back to the ecliptic (G2) and to the maximum northern latitude (G3).

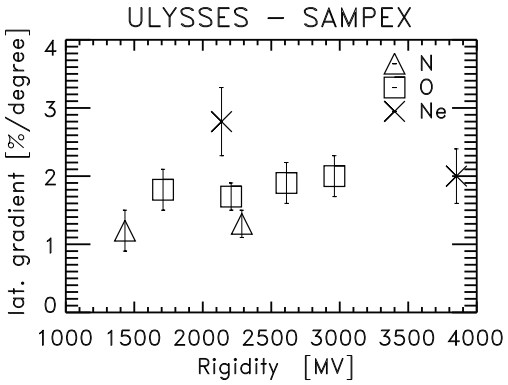

Fig. 7. Latitudinal gradients of nitrogen, oxygen and neon versus rigidity.

to 30 MeV/n), and extended the energy range for oxygen to 4 to 20 MeV/n. The Ulysses data survey reported here covers the period from launch in October 1990 until July 1995.

The data used in our survey have been separated into eight energy ranges. A complete list of the channels used can be found in Table 1. Intensity variations of the anomalous component due to solar modulation are taken into account by using SAMPEX data at 1 AU as reference measurements. These baselines were only available for four of our channels (see Table 1 and Fig. 4). To estimate baselines for the other four channels, we have extrapolated the known SAMPEX baselines. For example: by using Ulysses data from the ecliptic crossing in March 1995, we determined a Ulysses flux ratio for oxygen (8 to 12 MeV/n) to oxygen (4 to 8 MeV/n). This flux ratio was used to extrapolate the SAMPEX oxygen measurements (8 to 12 MeV/n) to 4 to 8 MeV/n, providing a baseline at this energy range. Since the flux ratios used for the extrapolation of the SAMPEX baselines are determined with data from a period when both satellites were in the ecliptic plane and at almost the same radial distance, we have eliminated radial and latitudinal effects on the intensities. This method further assumes that the spectral shape of the ACR is similar at both spacecraft which is the case for most of the current solar minimum. The only periods in question are in 1992 and 1993, where the low energy channels at Ulysses show contamination by solar energetic particles. These periods have been excluded from our survey.

After the decrease in solar activity in early 1992, the intensities recorded in all channels at Ulysses and SAMPEX showed a continuous increase. However, the increase was stronger at Ulysses until the spacecraft reached the maximum southern latitude. After passing the maximum southern latitude, the intensity at Ulysses decreased sharply and reached the SAMPEX value during the ecliptic crossing, followed by a sharp increase as Ulysses proceeded to high northern latitudes. This behaviour is as expected for a true latitudinal gradient.

After calculating the SAMPEX to Ulysses flux ratios for the three energy channels and plotting the results versus heliocentric ecliptic latitude, we found latitudinal gradients between 1% and 2% per degree. A summary of the gradients can be found in Fig. 6. Nitrogen latitudinal gradients are at about 1.2%, the oxygen gradients at about 1.8% while the neon gradients are somewhat higher but more uncertain. Note that these gradients are an average of individual gradients, determined for the data subsets G1, G2 and G3. This separation was necessary because of the observed north–south asymmetry in the heliosphere. During the ecliptic pass, the minimum flux intensity measured at Ulysses was reached at about 18°S, before the ecliptic was reached. We separated the data set into the three subsets, calculated the gradients and determined the final gradient by averaging the individual results.

Fig. 7 shows the latitudinal gradients plotted versus magnetic rigidity. This representation shows a weak tendency for the latitudinal gradient to increase with increasing rigidity.

The analysis of ACR data for the current solar minimum show positive latitudinal gradients. These observations together with negative latitudinal gradients (e.g., Stone 1987, Cummings et al. 1990) during times with reversed magnetic field direction of the former solar minimum give strong support to theories of particle propagation that include drifts in the large-scale magnetic field (e.g., Jokipii 1990). Comparing our results with other studies at the current solar minimum (e.g., Cummings et al. 1995b, Trattner et al. 1995b), we find similar latitudinal gradients for the oxygen channels used in these studies.

The latitudinal gradients may also be affected by the tilt of the current sheet. This suggestion was supported with observations by Cummings et al. (1990). During the current solar minimum, the tilt of the current sheet decreased from $\pm 30°$ in 1992 to $\pm 15°$ in 1995. No significant latitudinal gradient could be determined for the data subset G1 in 1992 until Ulysses reached about 30°S and moved completely into the polar coronal hole. However, stable latitudinal gradients over the complete latitudinal range could be determined for the data set in 1995 when

Ulysses experiences solar minimum conditions and a smaller tilt of the current sheet.

Another important subject is the observed heliospheric asymmetry. It was suggested by Kota and Jokipii (1983), that the wavy nature of the current sheet somewhat complicates the expected gradients. The gradients are modified by an assumed cross-field diffusion such that the minimum does not occur at the neutral sheet. However, Kota and Jokipii (1983) also suggested, that for periods when cosmic rays drift from the poles towards the ecliptic (as in the current solar minimum) they are less affected by the structure of the current sheet (i.e., inclination, waviness, regularity). During such periods the cosmic ray flux in the ecliptic should be almost constant. For periods when particles enter the heliosphere along the equatorial current sheet, they are strongly affected by the characteristics of the sheet.

Shea et al. (1986) reported a strong predominance of solar activity from the northern hemisphere of the sun from 1959 to 1970. This north–south asymmetry disappeared from 1971 to 1982. Since 1982 there was a predominance of flares in the southern hemisphere. It might be that this concentration of solar activity in one hemisphere causes different solar wind conditions within the two hemispheres which would be in turn effecting the observed asymmetry in the ACR latitudinal gradients. However, only longer investigations will allow to evaluate a trend of this behaviour.

The heliospheric asymmetry was also reported by Simpson et al. (1995b) and Goldstein et al. (1996). By following the intensity of the ACR (see e.g., Fig. 3), the flux at the maximum northern latitude is higher than the flux observed at the maximum southern latitude. Goldstein et al. (1996) pointed out, that the average solar wind speed in the northern hemisphere is about 2%–3% higher compared with the southern hemisphere. On the other hand, the solar wind density is reduced by 8% in the northern hemisphere causing a reduction in momentum flux of about 5%. Due to this reduced momentum flux, the heliosphere could be smaller in the northern hemisphere. We therefore would be closer to the source region of the ACR, the termination shock, which may be the source of the observed asymmetry in the ACR.

Acknowledgements. The authors would like to thank M.J. Szumlas and S.T. Ho from the Space Science Department of ESA for their support in processing the LET data. We acknowledge the use of the Ulysses Data System in the preparation of this paper. The HILT sensor on SAMPEX was supported by the Bundesministerium für Forschung und Technologie, FRG, under contract 50 OC 90021.

References

Balogh A., 1995, Nuclear Physics B – Proceedings Supplement Section, in press
Bame S.J., et al., 1993, Geophys. Res. Lett. 20, 2323
Bastian T.S., et al., 1979, Proc. 16th Int. Cosmic Ray Conf. 12, 338
Bothmer V., et al., 1995, Geophys. Res. Lett. 22, 3369
Christian, et al., 1995, App. J. 446, L105
Cummings A.C., Stone E.C., 1988, Proc. 6th Int. Solar Wind Conf. 2, 599
Cummings A.C., et al., 1990, Proc. 21st Int. Cosmic Ray Conf. 6, 206
Cummings A.C., et al., 1995a, Geophys. Res. Lett. 22, 341
Cummings A.C., et al., 1995b, Proc. 24th Int. Cosmic Ray Conf., in press
Fisk L.A., et al., 1974, Astrophys. J. 190, L35
Fisk L.A., 1986, in: The Sun and the Heliosphere in three Dimensions, ed. R.G. Marsden, Reidel, Dordrecht, p. 401
Forbush S.E., 1954, J. Geophys. Res. 59, 525
Goldstein B. E., et al., 1996, Astron. and Astrophys., this issue
Hasebe N., et al., 1994, Geophys. Res. Lett. 21, 3027
Hovestadt D., et al., 1973, Phys. Rev. Lett. 31, 650
Jokipii J.R., et al., 1977, Astrophys. J. 213, 861
Jokipii J.R., Davila J.M., 1981, Astrophys. J. 248, 1156
Jokipii J.R., Kota J., 1985, Proc. 19th Int. Cosmic Ray Conf. 4, 449
Jokipii J.R., 1990, in: Physics of the Outer Heliosphere, eds. S. Grzedzielski, D.E. Page, Cospar Colloq. Ser., Pergamon Press, NY, p. 169
Klecker B., 1977, J. Geophys. Res. 82, 5287
Klecker B., et al., 1993, IEEE Trans. Geosci. Remote Sensing 31, 542
Klecker B., et al., 1995, Ap. J. 442, L69-L72
Kota J., Jokipii J.R., 1983, Astrophys. J. 265, 573
Marsden R.G., et al., 1986, in: The Sun and the Heliosphere in three Dimensions, ed. R.G. Marsden, Reidel, Dordrecht, p. 477
Marsden, R.G., et al., 1996, Astron. and Astrophys., this issue
McDonald, et al., 1995, Ap. J. 446, L101
McKibben R.B., et al., 1995, Space Science Rev. 72, 367
Mewaldt R.A., et al., 1993, Geophys. Res. Lett. 20, 2263
Möbius E., et al., 1985, Nature 318, 426
Page D.E., 1975, Science 190, 845
Pesses M.E., et al., 1981, Astrophys. J. 246, L85
Phillips J.L., et al., 1995, Geophys. Res. Lett. 22, 3301
Potgieter, M.S., 1985, Proc. 19th Int. Cosmic Ray Conf. 4, 425
von Rosenvinge T.T., McDonald F.B., 1975, Proc. 14th Int. Cosmic Ray Conf. 2, 792
Sanderson T.R., et al., 1995, Geophys. Res. Lett. 22, 3357
Shea M.A., et al., 1986, in: The Sun and the Heliosphere in three Dimensions, ed. R.G. Marsden, p. 395-400
Simpson J.A., 1989, Adv. Space Res. 64, 1691
Simpson J.A., et al., 1992, Astron. and Astrophys. 92, 365
Simpson J.A., et al., 1995a, Science 268, 1019
Simpson J.A., et al., 1995b, EOS Transaction F457
Smith E.J., et al., 1995, Geophys. Res. Lett. 22, 3325
Stone E.C., 1987, Proc. 20th Int. Cosmic Ray. Conf. 7, 105
Stone E.C., et al., 1987, EOS Trans., AGU 68, 1413
Trattner K.J., et al., 1995a, Geophys. Res. Lett. 22, 337
Trattner K.J., et al., 1995b, Geophys. Res. Lett. 22, 3349
Webber W.R., et al., 1981, Proc. 17th Int. Cosmic Ray Conf. 10, 92
Wenzel K.-P., et al., 1989, Adv. Space Res. 9, 25